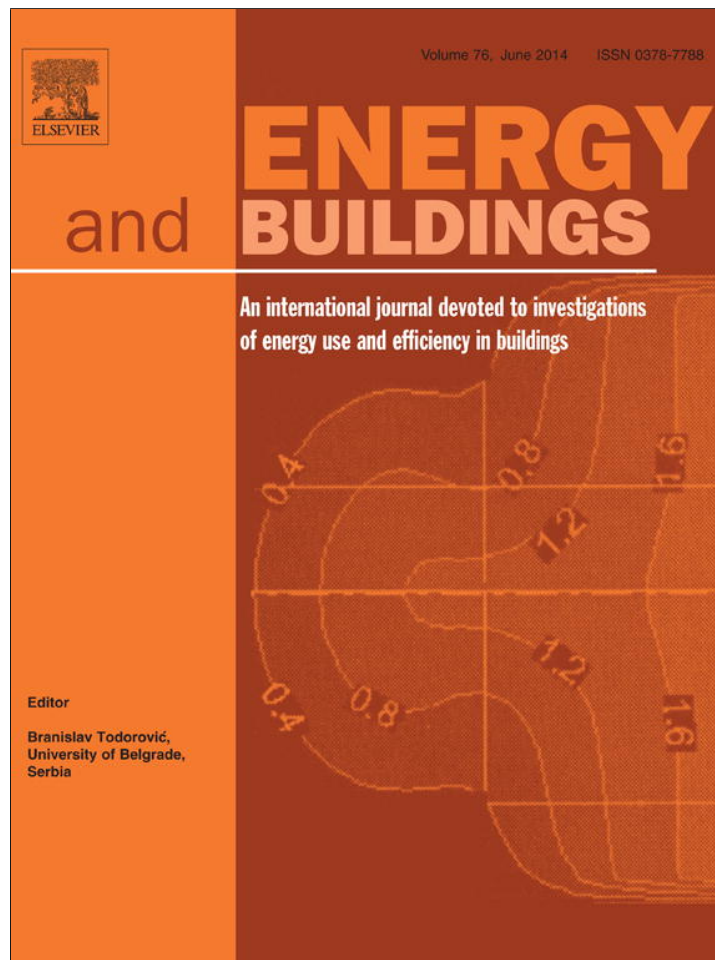


Provided for non-commercial research and education use.
Not for reproduction, distribution or commercial use.



This article appeared in a journal published by Elsevier. The attached copy is furnished to the author for internal non-commercial research and education use, including for instruction at the authors institution and sharing with colleagues.

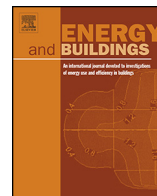
Other uses, including reproduction and distribution, or selling or licensing copies, or posting to personal, institutional or third party websites are prohibited.

In most cases authors are permitted to post their version of the article (e.g. in Word or Tex form) to their personal website or institutional repository. Authors requiring further information regarding Elsevier's archiving and manuscript policies are encouraged to visit:

<http://www.elsevier.com/authorsrights>

Contents lists available at [ScienceDirect](http://www.sciencedirect.com)

Energy and Buildings

journal homepage: www.elsevier.com/locate/enbuild

Improving the capabilities of the Town Energy Balance model with up-to-date building energy simulation algorithms: an application to a set of representative buildings in Paris

G. Pigeon^{a,*}, K. Zibouche^b, B. Bueno^c, J. Le Bras^a, V. Masson^a^a CNRM-GAME, URA1357, CNRS – Météo, Toulouse, France^b Université Paris-Est, Centre Scientifique et Technique du Bâtiment (CSTB), France^c Massachusetts Institute of Technology, Cambridge, MA, USA

ARTICLE INFO

Article history:

Received 18 April 2013

Received in revised form 25 October 2013

Accepted 26 October 2013

Available online 19 February 2014

Keywords:

Urban Climate Model

Building Energy Model

ABSTRACT

Buildings' energy systems release heat to the atmosphere that contributes to the urban heat island. In return, the energy demand from buildings depends on the meteorological conditions of their surroundings. Consequently, urban canopy models such as Town Energy Budget (TEB) have progressively included the representation of the main processes of building energetics: solar and internal heat gains, heat transmission through the enclosure and the heat exchange by infiltration and ventilation. The objective of this study is to extend the evaluation of the Building Energy Model (BEM) implemented in TEB. Five buildings representative of the morphological and thermal characteristics that can be encountered in European urban areas have been selected. The evaluation has been conducted with EnergyPlus building energy model and for two contrasted climates. The TEB model is able to estimate the heating and the cooling energy demand with an accuracy better than 5 kWh/m²/year for heating and 3 kWh/m²/year for cooling. This paper also discusses on the importance of computing the building's surrounding surface temperature for energy demand calculations. TEB is able to account for this effect whereas EnergyPlus assumes that building surroundings are at air temperature.

© 2014 Elsevier B.V. All rights reserved.

1. Introduction

The releases of heat by buildings in urban areas are an additional source of energy in comparison to most of other environments and are one of the causes leading to the urban heat island phenomenon. These releases can be dominated by the use of energy for space heating during the winter period [1,2] but, generally, the releases by air cooling condensers have retained most of the attention. The impact of the massive use of air cooling systems in Asian and North-American cities has been documented in the literature, for example in Houston City (Texas) [3] and in Tokyo [4]. In both studies, an increase of night temperatures up to 2 °C has been calculated using a numerical method based on a building energy model and an urban canopy model coupled with a mesoscale atmospheric model. Whereas the use of air cooling systems is not currently spread out

in all types of climates and cities such as in mid-latitude Europe, the use of these systems is expected to increase in response to higher standards of living requirements and the climate warming. In France, a doubling of the energy consumption due to air conditioners is expected by 2030 [5]. Based on these figures, De Munck et al. [6] have estimated an increase in the urban heat island of 2 °C over Paris while they estimated the current impact of air cooling condensers to be 0.5 °C.

At the same time, the energy demand of buildings responds to climate variation of their environment. In the case of urban areas with a high level of air cooling systems, the increase of temperature leads to an increase in the energy demand. For example in Tokyo, Ohashi et al. [7] reported an increase of 1.6 GW per degree of the outdoor air temperature. Based on numerical simulations, Bueno et al. [8] reported that the urban climate mainly influences the energy performance by the process of infiltration and ventilation and that a 5% increase in cooling energy demand can be expected per degree increase of air temperature for residential buildings (historical collective) and a similar decrease in heating energy demand of a residential building can be expected for the

* Corresponding author at: 42 av. Coriolis, 31057 Toulouse Cedex, France. Tel.: +33 0 561078381.

E-mail address: gregoire.pigeon@meteo.fr (G. Pigeon).

wintertime period (temperate climate). Consequently, the knowledge of the intensity of the urban heat island is of interest for the energy design of buildings in urban areas and some methods have recently been developed [9] to respond to this purpose. In urban planning, there is also a demand for building stock models to assist with the implementation of policy. Swan and Ugursal [10] review the various modelling techniques used to estimate the energy consumption at neighbourhood or city scale. The top-down approach utilizes historic aggregate energy data, deriving the energy consumption of building stocks as a function of top-level variables such as macroeconomic indicators, energy price, and general climate. Bottom-up models account for the energy consumption of individual end-users and extrapolate it to represent an urban area based on the representative weight of the modelled sample. A number of physically-based bottom-up models can be found in the literature [11]. However, none of these models specifically accounts for the interactions between buildings and the urban environment. The Urban Canopy and Building Energy Models (UC-BEMs) can overcome this limitation and have the potential to become fully-operative building stock models.

The Town Energy Budget (TEB) model [12] has been recently modified by adding a Building Energy Model (BEM) [13]. TEB proposes a physically-based (bottom-up) approach to estimate building energy consumption at city scale (~10 km) with a resolution of a neighbourhood (~100 m). Modelling building energy consumption at urban scale has the advantage of building aggregation but requires taking into account the energy interactions between buildings and the urban environment. Building aggregation allows the simplification of the building thermal definition. The underlying assumption is that the average building of a certain urban area is more representative and generic than each particular building. The main hypotheses adopted in this new component of TEB have been evaluated using a numerical model specifically dedicated to building energy use. Then, the new version of TEB has been evaluated against observations, as it was done before for previous versions of TEB [14,15]. As for every numerical model, the evaluation of urban canopy layer models is a critical step before they can be used inside mesoscale, regional or global climate atmospheric models. In this sense, a recent international exercise has been conducted for a large number of them [16,17] for a residential suburban area. However, given the heterogeneity of the urban environment and the large number of building types that compose the urban landscape, the work of evaluation of such models is still necessary to estimate their ability to reproduce the urban climate and to estimate their level of precision.

Given these considerations on the urban climate and the Urban Climate Models, the objective of this study is to complete the evaluation of the TEB model for a set of buildings representative of the Paris area. This set of buildings includes different kinds of morphology and envelope. The study is based on comparisons with the EnergyPlus building energy model [18]. Indeed, the real energy consumptions of buildings are difficult to use for this purpose since they are strongly influenced by the behaviour of the dwellers and other information about the building that are often unknown and that can have large variations from one building to another. For that reason, the use of a numerical benchmark such as EnergyPlus is a better alternative since it has been validated against controlled buildings equipped with sensors. The paper describes, first, the general methodology adopted in the study and, then, the set of buildings selected. The different modifications implemented in the TEB model are presented before the results. Based on the use of the TEB model, the sensitivity of the model to the surface temperature of the surrounding used in the longwave infrared balance of the wall is presented.

2. Modelling differences between TEB and EnergyPlus

During this study, the differences between TEB and EnergyPlus have been considered and some improvements have been implemented in the BEM module. Since the improving of TEB is the objective of this study, a brief description of this model is presented and then the differences with the EnergyPlus model that have been investigated.

2.1 TEB brief description

The TEB model has been developed to simulate the energy and water exchanges between the city and the atmosphere. The most important processes that influence urban-atmosphere energy exchanges are taken into account in TEB, viz:

- radiative trapping and shadows resulting from the 3D geometry of a city;
- heat exchanges between the buildings and the environment;
- water interception and evaporation, and also snow mantle evolution on roads and roofs (evaluated against Montreal data [15]);
- drag, heat and water turbulent exchanges between the urban canopy layer and the atmosphere.

Meanwhile, the parameterization conceptualization allows fast computation time. For example:

- The 3D shape of a city is parameterized by an idealized 2D canyon geometry while keeping the main features driving the radiative interactions and the energy exchanges [12].
- Likewise, energy balance computations are carried out by azimuthal averaging solar and wind forcing in order to represent neighbourhoods with random-oriented urban canyons. For impact studies, a version of the model with specific canyon orientations is also available [19].
- The air flow within urban canyons is solved by applying aerodynamic resistances and, in the latest version, by applying an original 1D vertical turbulence scheme that simulates the mean characteristics of the flow in the canyon, skipping unnecessary (and computationally expensive) details [20].

The BEM [13] implemented in TEB considers a single thermal zone, a generic thermal mass to represent the thermal inertia of the indoor materials, the heat gains resulting from transmitted solar radiation and the internal sources of heat, infiltration and ventilation. The heat conduction through the envelope of the building is calculated using a finite difference method individually for each surface (roof, wall and floor). The morphological parameters of the TEB model are summarized in Table 1.

2.2 Sky model

The first difference concerns the representation of the diffuse solar radiation from the sky. In the original version of the BEM implemented in TEB, the diffuse solar radiation has no directional effect and each surface of the canyon receives this energy flux according to its sky view factor. In EnergyPlus a more detailed sky radiance model is applied and the diffuse radiation is not isotropic. When comparing both models, it resulted in an overestimation of the total solar radiation received by the wall around midday in TEB (Fig. 1, points) driven by the contribution of the diffuse solar radiation. On average, during the summer period (future climate), the overestimation was about 12 W/m² which represents more than 7% of the solar heat flux. Consequently, the calculation of the diffuse solar radiation has been modified in TEB. The contribution of the circumsolar brightening, which is the diffuse solar radiation

Table 1
TEB morphological parameters.

Symbol	description	unit	Diagram and equations
Input parameters			
λ_{BLD}	Building plan area density	-	
W_o_H	Wall-to-horizontal urban area ratio	-	
GR	Façade glazing ratio	-	
h_{BLD}	Building height	m	
h_{FLOOR}	Floor height	m	
Deduced parameters			$\lambda_{BLD} = \frac{A_{BLD}}{A_{URB}} \quad W_o_H = \frac{A_{WALL}}{A_{URB}} \quad GR = \frac{A_{WIN}}{A_{WALL}}$ $W_o_B = \frac{A_{WALL}}{A_{BLD}} \quad G_o_B = \frac{A_{WIN}}{A_{BLD}} \quad M_o_B = \frac{A_{MASS}}{A_{BLD}}$
W_o_B	Wall-to-horizontal building area ratio	-	
G_o_B	Glazing-to-horizontal building area ratio	-	
M_o_B	Mass-to-horizontal building area ratio	-	

concentrated around the sun, has been estimated as in EnergyPlus [21, pp. 142–143]. This fraction of the diffuse solar radiation is now treated as the direct solar radiation. This modification resulted in a better representation of the total solar radiation received by the wall (Fig. 1, triangles). On average, for the summer period, the wall in both models receives the same amount of energy per unit of surface since the difference is -0.03 W/m^2 .

2.3 Window optical properties

The second difference is the calculation of the optical properties of the windows with the Solar Heat Gain Coefficient (SHGC) and the window conductance (U factor). Comparing TEB with EnergyPlus, we found that TEB tends to transmit more solar radiation into the building than EnergyPlus. This bias resulted from an overestimation of the glazing transmittance properties in the original version (Table 2). For single glazing windows, EnergyPlus estimated a transmittance of 0.22 while it is 0.33 for TEB. For other windows better insulated the difference was lower. The other optical properties of the windows were also affected and for example, in the case of the double glazing windows, the absorptance calculated with TEB was almost twice the value calculated by EnergyPlus. It resulted for the buildings that have such windows in an overestimation of the window's outdoor surface temperature. To correct this bias, the calculation of the properties of the glazing has been modified and it is now based on an adaptation of the simple window model described in the Engineering Reference documentation of EnergyPlus [21, pp. 217–222]. In the TEB, the calculation is now done in two steps:

- The transmittance and the reflectance at normal incidence are calculated based on the values of U factor and SHGC.
- These two properties are corrected by two fixed coefficients (one for each property) to take into account the variability of the solar radiation angles of incidence on the glass during one year, for various latitude and for various street orientation. These coefficients are computed as averages of the transmittance and reflectance factors for angles of incidence between 18 and 72° with a step of 9° .

The optical properties resulting from this modification of TEB are presented in Table 2 and are closer to EnergyPlus estimates than the properties originally calculated. For any transmittance, reflectance and absorptance, the difference between both models is never higher

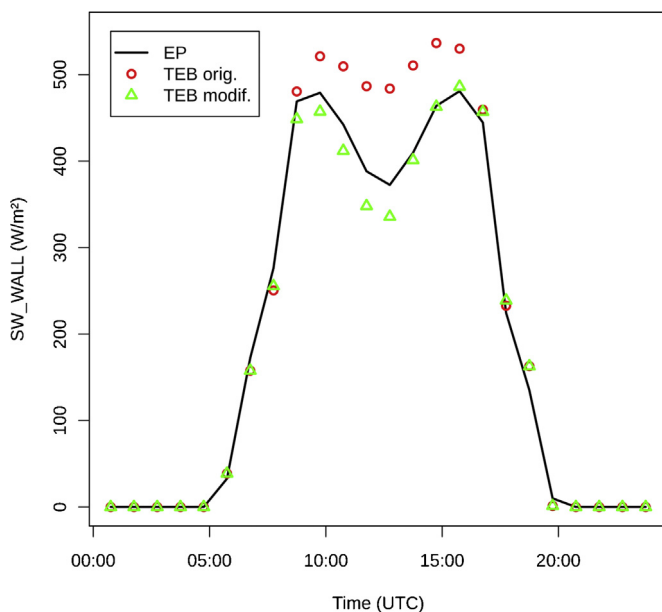


Fig. 1. Total solar radiation received by the walls (average of the different walls) during a sunny summer day for future possible climate conditions (latitude of $37^\circ 50' \text{ N}$) with EnergyPlus (solid line), the original version of TEB (circles) and the modified version (triangles).

Table 2
Averaged optical properties of the windows for EnergyPlus, the original and the modified version of TEB for the 3 types of glazing simulated.

Rad. properties Model	Transmittance			Reflectance			Absorbance		
	EP	ori. TEB	mod. TEB	EP	ori. TEB	mod. TEB	EP	ori. TEB	mod. TEB
Single pane windows U factor = 4.95 Wm ⁻² K ⁻¹ SHGC = 0.425	0.22	0.33	0.23	0.34	0.14	0.33	0.43	0.53	0.44
Double pane windows. Low insulation. U factor = 2.4 Wm ⁻² K ⁻¹ SHGC = 0.425	0.27	0.33	0.28	0.60	0.46	0.60	0.13	0.21	0.12
Double pane windows. High insulation. U factor = 1.95 Wm ⁻² K ⁻¹ SHGC = 0.425	0.27	0.33	0.28	0.61	0.47	0.61	0.11	0.20	0.10

than 0.01. Concerning the window's energy budget, in the original version, only the outdoor layer was absorbing solar energy. It often resulted in an underestimation of the indoor surface temperature of the window. The solar absorption is now equally distributed over both layers.

2.4 Convective heat transfer coefficient

The third difference is the calculation of the Convective Heat Transfer Coefficient (CHTC) at the outside layers of the building. These coefficients are crucial for estimating the turbulent convective heat fluxes and the energy demand of buildings. However, they are difficult to estimate and a large variety of formulations exist [22,23] based on the wind speed at a reference location and the temperature difference between the surface and the air. The reported relations are empirical and mostly linear-laws such as the relation used in TEB [24,25] or power-laws. Compared to the DOE-2 algorithm [21, p. 68] used in EnergyPlus for this study, the CHTC of TEB is 2.5 times higher (Fig. 2) which induces differences on the wall surface temperature up to 5 K. In the case of buildings with low insulation level of the wall, this difference impacts significantly the energy demand. For the roof, the differences between the TEB original formulation [26] and the DOE-2 algorithm are lower but TEB

computes CHTC up to 60% higher (Fig. 2). The DOE-2 formulations have been implemented and are a new option in the TEB model for both the wall and the roof. This formulation, originally, includes a dependency on the wind direction respective to the surface. However, in an urban environment at the neighbourhood scale (~100 m) for which the TEB model is designed, many wall directions generally coexist. Consequently, the CHTC adopted is calculated as the average of the leeward and the windward formulation.

For the convective heat exchange within the building, the original version of TEB used constant coefficients. By comparing simulations using a constant formulation and simulations using the TARP algorithm [21, pp. 89–90], differences of the energy demand up to 10% were observed. During the simulation of the Simplified Model (see Section 3) with EnergyPlus, the coefficients for the roof ranged between 1 and 2.5 W/(m² K) while regularly reached 4.4 W/(m² K) in TEB. Similarly, the coefficient for the walls in TEB was constant 3.076 W/(m² K) whereas it varies between 1 and 2.5 W/(m² K) in the case of EnergyPlus. The formulation proposed in the TARP algorithm has been implemented in the TEB model as a new option for the purpose of this comparison. However, as suggested by different reviews [22,23], it is not clear that one formulation is really better than the others.

2.5 Environment surface temperatures for the longwave radiation balance

Another difference between both models is the representation of the building's surrounding surface temperatures used in the longwave radiation balance. In TEB, the surface temperature of the opposite wall and the road are calculated and used for the calculation of the longwave heat balance of one wall. In EnergyPlus, the opposite wall and the road surface temperature are approximated by the air temperature. Both models also receive the downwelling longwave radiation from the sky. But while this longwave exchange with the sky should be directly proportional to the wall sky-view factor, in EnergyPlus a certain fraction of the heat exchange is computed with the air temperature [21]. The same calculation has been implemented in TEB for this study and the sensitivity to the representation of the surrounding surface temperatures will be discussed in Section 4.

3. Model comparison for a set of representative buildings in Paris

3.1 General description of the method

In order to assess the accuracy of our model, a two-step methodology has been applied (Fig. 3):

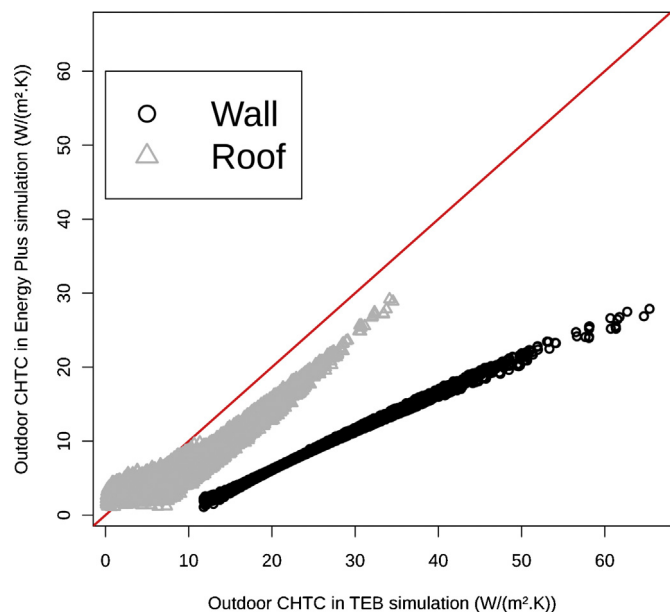


Fig. 2. Scatterplots of the convective heat transfer coefficients (CHTC) for the outside surface of the wall (circles) and the roof (triangles) for TEB (x-axis) and EnergyPlus (y-axis) in the case of the present climate simulation for the Historical collective building.

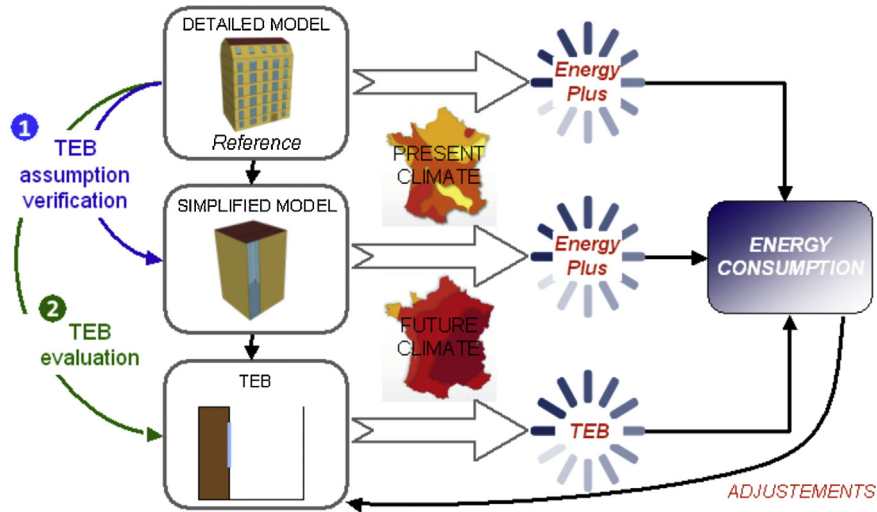


Fig. 3. Diagram of the methodology developed to evaluate the TEB model.

- The first step aims at assessing the level of accuracy that can be reached with a building representation as simple as the one of the TEB model. The method is based, as in Bueno et al. [13], on the comparison of the energy demand simulated with the EnergyPlus numerical model for the same building but with two different levels of details. For each type of building, a detailed model (DM) is simulated with a precise geometry describing the morphology of the envelope, each floor of the building as a separate thermal zone, the exact location of the windows in these thermal zones, the shape of the roof and the existence of attic when necessary. Then, a simplified model (SM) is build according to the main assumptions of the TEB model (single thermal zone, unique thermal mass, uniform glazing ratio). Since the DM can have any plan area shape, it is simulated on eight different orientations separated by 45°. The SM, which has a square ground, is simulated for two directions (Fig. 4). The energy demand calculated for both models are compared. From this first step, it has been possible to assess the level of precision that could be achieved by the simplification of the building morphology and to quantify the improvements that could be gained with a better description of the building geometry.
 - For the second step, the same building is simulated with the TEB model and the energy demand is compared with the DM in order to assess the level of accuracy of TEB with respect to EnergyPlus and to evaluate the main differences between both models (Fig. 3). During this step, comparisons with the results of the SM have been carried out in order to understand the origin of the differences between the models.
- To verify the precision obtained with the SM and the TEB model to represent the energy demand for heating and cooling, the two steps are applied for the present climate condition of Paris and for a possible future climate of the same area. The meteorological conditions of the present climate are extracted from the weather data file of Paris-Orly collected by ASHRAE [27] and available from the EnergyPlus website (<http://apps1.eere.energy.gov/buildings/energyplus/weatherdata.about.cfm>). In the light of the results from Hallegatte et al. [28], a future possible climate for Paris region is analogous to the current conditions for Cordoba (Spain). Consequently, the data gathered for this city in the Spanish Weather for Energy Calculations data set were used. In the present climate conditions

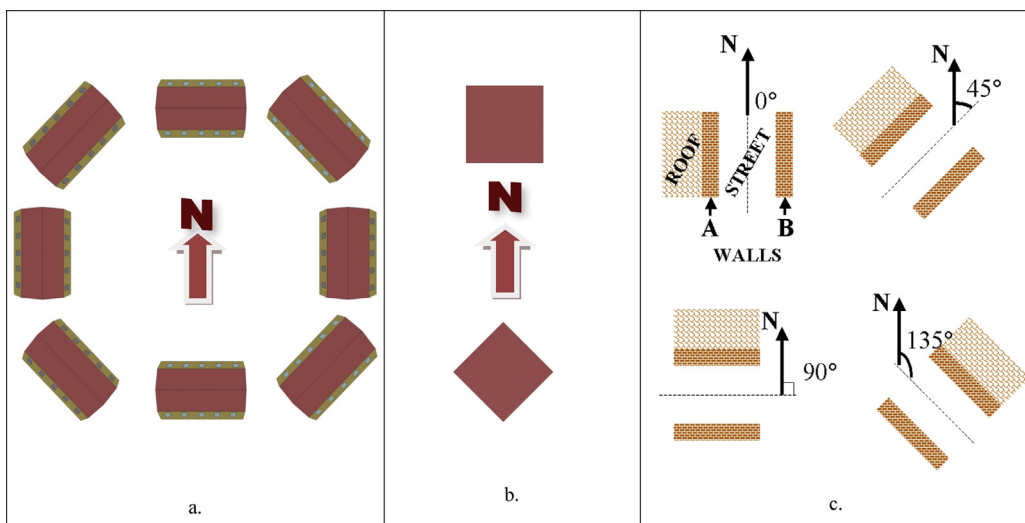


Fig. 4. The different orientations adopted for the different models: (a) the detailed building model simulated for 8 orientations with EnergyPlus, (b) the simplified building model simulated for 2 orientations with EnergyPlus and (c) the configuration adopted for the TEB model.

Table 3
Morphological, indoor and window properties of the five building types.

Description	Symbol	Unit	Historical coll.	Post war coll.	High rise tower	Old detached house	Recent detached house
<i>Morphology</i>							
Length of the side of the square building plan		m	27.4	16.3	20.4	5.8	9.3
Wall to urban area ratio	$W_{o.H}$		0.0031	0.0082	0.0216	0.0038	0.0012
Façade glazing ratio	GR		0.19	0.34	0.34	0.06	0.07
Building height	h_{BLD}	m	21.5	33.5	110.2	5.6	2.72
<i>Heat gains</i>							
Internal heat gains		$Wm^{-2}[\text{floor}]$	4.43	4.43	4.43	4.43	4.43
Radiant fraction of internal heat gains			0.412	0.407	0.403	0.413	0.407
Latent fraction of internal heat gains			0.175	0.186	0.193	0.174	0.186
<i>Windows</i>							
Window solar heat gain coefficient	SHGC		0.425	0.425	0.425	0.425	0.425
Window U-factor	U factor	$Wm^{-2} K^{-1}$	4.95	2.40	2.40	4.95	1.95
Floor height	h_{FLOOR}	m	3.07	3.05	2.90	2.80	2.72
<i>Infiltration</i>							
Infiltration rate		ACH	0.52	0.54	0.55	0.54	0.52

of Paris, the building energy consumption is heating-dominated while in the present climate conditions of Cordoda, it is cooling-dominated. Consequently, using both sites, it is possible to have a wide range of climate conditions and building behaviour.

3.2 Description of the building simulations with TEB

As mentioned, in the second step of the evaluation, the same set of representative buildings have been represented with the TEB model. In that model, the morphology is defined as a generic urban canyon whereas, in EnergyPlus, isolated buildings are described. To overcome this difference, the inputs of the TEB simulations concerning the morphology of the buildings and the environment meteorological variables have been chosen carefully so that the comparison between EnergyPlus and TEB can give information about the precision of the BEM included inside the model.

First, the TEB morphological variables (Table 1) have been calculated to represent a single building, isolated from other buildings such as in the EnergyPlus simulations run for this study. However, the basic geometry of TEB is a street canyon with 2 opposite walls for which the main parameters are the plan area density of buildings (λ_{BLD}) and the wall area to horizontal urban area ratio ($W_{o.H}$). Nevertheless, assuming a low value for λ_{BLD} such as 10^{-3} , it is possible to reduce the view factors between the two opposite walls of the canyon for almost any value of $W_{o.H}$. As an example, for a high building with a ratio between its wall surface and its horizontal built surface ($W_{o.B}$) of 20, the view factor of the opposite walls is only 0.003 against a null value for an isolated building. Consequently a fixed value of 10^{-3} has been chosen for λ_{BLD} for all buildings. Then, the other morphological parameter of TEB, $W_{o.H}$, has been calculated in order to conserve the $W_{o.B}$ ratio of the simple and detailed models:

$$W_{o.H} = W_{o.B} \times \lambda_{BLD} \quad (1)$$

and to have the same surface exchange of the building with the outdoor. The glazing ratio per unit wall area (GR) is calculated so as to conserve the glazing ratio per unit built area ($G_{o.B}$). The roof of the TEB model is flat and the building height that defines the building air volume to be heated or cooled is conserved. For those buildings that have a pitched roof (see Section 3.4) and for which the roof space is not conditioned, the height is taken at the base of the roof. The floor height is calculated to have the same number of floors as in the detailed model. With this assumption, the TEB

model will automatically computes an equivalent area of thermal mass inside the building as in the detailed and simple models. In the latest version of the TEB model, it is possible to describe the street orientations and to have a specific energy balance for the 2 opposite walls of the street canyon [19]. This option have been activated so to have a representation very similar to that EnergyPlus (Fig. 4).

The building materials used in the simulations are identical in EnergyPlus and in TEB (Tables 3 and 4). When air layers are present, they are prescribed in EnergyPlus with a thermal resistance. In TEB, the thickness and the thermal conductivity that defines each material are adapted to conserve the thermal resistance. The window properties are the same as in the EnergyPlus simulations. Finally, the internal heat gains and the infiltration flow rate are also conserved from the detailed and simple models.

The TEB model is run in a stand-alone mode using meteorological data [14]. Generally, these data are the boundary conditions above the canopy layer and the TEB model computes the air temperature and the wind speed inside the canyon depending of the drag and the energy balance. However, in this study the objective is to evaluate the precision of the BEM included inside TEB and not the differences that depends on the urban climate calculation. Consequently the same corrections as in EnergyPlus have been applied to determine the air temperature and the wind inside the street. For the temperature, the correction is done according to the dry adiabatic lapse rate [29] and the height of the building. For the wind, it depends on the roughness of the urban context. Consequently, the same environmental meteorological data as in EnergyPlus simulation has been applied at the roof level.

3.3 Building set description

Five buildings have been selected to be representative of Paris urban area and are presented in Fig. 5. The characteristics of the buildings are from former studies or technical notes [30–32].

The first one is an historical collective building which covers over 75% of the buildings present inside the city of Paris. These buildings are generally adjoined in blocks. They were typically built before 1900 with a thick street façade wall in limestone whereas the courtyard façade wall was in brick. They typically have 5–7 floors and the tin roofing has two different slopes. Because of the high housing demand in Paris, the roof space has been generally converted and is occupied. Most of these buildings are poorly insulated.

Table 4
Roof, wall and floor thermal properties for the five building types.

a. Historical collective building						
Description Unit	Material	Thickness m	Volumetric heat capacity $J m^{-3} K^{-1}$	Thermal conductivity $W m^{-1} K^{-1}$	Albedo	Emissivity
<i>Roof</i>						
Layer 1 (out)	Zinc	0.0008	2736000	110.00	0.4	0.9
Layer 2	Wood	0.0150	900000	0.18		
Layer 3	Air layer	0.0050	1210	0.06		
Layer 4	Wood and plaster mix	0.0150	1800000	0.80		
Layer 5	Air layer	0.0100	1210	0.07		
Layer 6 (in)	Wood	0.2000	800000	0.29		
<i>WALL</i>						
Layer 1	rock and brick mix	0.3000	1913396	1.04	0.4	0.9
<i>FLOOR</i>						
Layer 1	Wood	0.2000	800000	0.29		
b. Post war collective building						
Description Unit	Material	Thickness m	Volumetric heat capacity $J m^{-3} K^{-1}$	Thermal conductivity $W m^{-1} K^{-1}$	Albedo	Emissivity
<i>Roof</i>						
Layer 1 (out)	Gravel	0.0500	1800000	2.00	0.4	0.9
Layer 2	Asphalt	0.0200	2373500	1.00		
Layer 3	Insulation	0.0400	52030	0.03		
Layer 4 (in)	Concrete	0.2200	2016000	1.95		
<i>Wall</i>						
Layer 1	concrete	0.2200	2016000	1.95	0.4	0.9
<i>Floor</i>						
Layer 1	Concrete	0.2200	2016000	1.95		
c. High rise tower						
Description Unit	Material	Thickness m	Volumetric heat capacity $J m^{-3} K^{-1}$	Thermal conductivity $W m^{-1} K^{-1}$	Albedo	Emissivity
<i>Roof</i>						
Layer 1 (out)	Gravel	0.0500	1800000	2.00	0.4	0.9
Layer 2	Asphalt	0.0200	2373500	1.00		
Layer 3	Insulation	0.0400	54450	0.03		
Layer 4 (in)	Concrete	0.1500	2016000	1.95		
<i>Wall</i>						
Layer 1 (out)	Concrete and gravel mix	0.0700	2016000	1.95	0.4	0.9
Layer 2	Insulation	0.0400	54450	0.03		
Layer 3 (in)	plaster	0.0600	1800000	0.8		
<i>Floor</i>						
Layer 1	Concrete	0.2000	2016000	1.95		
d. Old detached house						
Description UNIT	Material	Thickness m	Volumetric heat capacity $J m^{-3} K^{-1}$	Thermal conductivity $W m^{-1} K^{-1}$	Albedo	Emissivity
<i>Roof</i>						
Layer 1 (out)	Red tiles	0.0250	1600000	1.00	0.2	0.9
Layer 2	Wood	0.0150	900000	0.18		
Layer 3	Air layer	0.0050	1210	0.06		
Layer 4	Wood and plaster mix	0.0150	1800000	0.29		
Layer 5	Air layer	0.0500	1210	0.28		
Layer 6 (in)	wood	0.2000	1800000	0.29		
<i>Wall</i>						
Layer 1 (out)	Millstone	0.3850	2200000	1.70	0.4	0.9
Layer 2 (in)	Plaster	0.0150	1800000	0.80		
<i>Floor</i>						
Layer 1	Wood	0.2000	800000	0.29		
e. Recent detached house						
Description Unit	Material	Thickness m	Volumetric heat capacity $J m^{-3} K^{-1}$	Thermal conductivity $W m^{-1} K^{-1}$	Albedo	Emissivity
<i>Roof</i>						
Layer 1 (out)	Concrete tiles	0.0100	1980000	1.95	0.3	0.9
Layer 2	Wood	0.0150	650000	0.18		
Layer 3	Air layer	0.0100	1210	0.06		
Layer 4	insulation	0.1000	50750	0.04		
Layer 5 (in)	plaster	0.0130	632000	0.33		
<i>Wall</i>						
Layer 1 (out)	Coating	0.0120	1800000	1.15	0.4	0.9
Layer 2	Breeze-block	0.2000	845000	1.05		

Table 4
Roof, wall and floor thermal properties for the five building types.

e. Recent detached house

Description Unit	Material	Thickness m	Volumetric heat capacity $J m^{-3} K^{-1}$	Thermal conductivity $W m^{-1} K^{-1}$	Albedo	Emissivity
Layer 3	Insulation	0.1000	50750	0.04		
Layer 4 (in)	Plaster	0.0130	632000	0.33		
<i>Floor</i>						
Layer 1 (in)	Concrete	0.0800	1980000	1.95		
Layer 2 (out)	Polystyrene	0.1200	26000	0.04		

Table 5
Sensitivity of the energy demand to the specific description of the building conducted with EnergyPlus.

		Heating (present climate)		Cooling (future climate)	
		Absolute difference (kWh/m ² [floor])	Relative difference (%)	Absolute difference (kWh/m ² [floor])	Relative difference (%)
Infiltration/ventilation: dynamic vs. static	Hist. Coll.	2.85	4	0.24	2
	Recent det. house	0.07	0	0.02	0
Roof ventilation	Recent det. House	-0.22	-1	-0.13	-1
Roof shape	Hist. coll.	-1.40	-2	-0.01	0
	Recent det. house	0.23	1	-0.40	-3
Two zones vs single zone building	Hist. coll.	-0.94	-1	-0.13	-1
Seven zones vs single zone building	Hist. coll.	-2.52	-3	-0.79	-4

The second type is a post war collective building (5% over Paris) with eleven floors. These were built rapidly with beams filled in-between by concrete. The thermal insulation of these buildings is also generally poor and since they are arranged individually without parted walls they have stronger energy demand than the historical buildings. Moreover, the glass surfaces were increased without any considerations for energy savings.

The third type of buildings are high rise tower built around the 1970's. The typical height of these buildings ranges between 80 and 110 m with up to 30 floors. Their construction started to adopt the use of insulation material for the roof and the wall. It resulted in a decrease in the energy demand. Such as the post collective buildings, the high rise towers have a large ratio of glazing over their façade and the buildings were isolated from each other. Given the particularly svelte geometry of this building, the DM solves only three storeys (top, ground and intermediate), assuming that all intermediate storeys have the same thermal conditions, so that the floor and ceiling of one storey can be considered adiabatic. Fig. 5 presents only this intermediate floor.

Finally, two individual houses have been selected since they represent a large part of the housing in the suburban areas of Paris. First, an old detached house also built during the post war period and before the adoption of the first rule for energy savings in 1974.

This house has two storeys with uninsulated thick walls. The walls are built with the typical millstone from the region in the south of Paris. It has the typical pitched roof which is not insulated. Concerning the glazing, they are also of poor thermal quality with a high conductance level.

The second house chosen is a recent one, which adopts one of the most recent rules concerning the thermal performance of the buildings. Consequently, the pitched-roof and the wall are insulated and the glazing has also good insulation properties. This is also a single-floor house and the roof structure is lighter than for the old detached house. The characteristics of each building are presented in Tables 3 and 4. This selection covers a wide range of buildings with different morphology. For example the ratio of the wall envelope to the ground surface of the buildings varies between 1.2 and 21.6, the glazing ratio between 6 and 34% of the façade. The thermal properties of the roofs and the walls also cover a wide range from non-insulated constructions to the use of thick insulation layers.

3.4 Results of the comparison between the detailed and the simplified models with EnergyPlus

First, the sensitivity of the energy demand to a reduced set of properties of the buildings has been evaluated. This analysis has

Table 6
Comparison of the heating demand between the simplified and the detailed model simulated with EnergyPlus.

Climate	Building type	Detailed model energy demand kWh/m ² [floor]/year	Absolute difference (simpl.-detailed) kWh/m ² [floor]/year	Relative difference (simpl.-detailed) %
Present climate	Historical collective	79.76	-5.12	-6
	Post war collective	112.75	0.75	1
	High rise tower	43.10	2.03	5
	Old detached house	211.78	3.11	1
	Recent detached house	49.19	1.19	2
Future climate	Historical collective	22.33	-0.80	-4
	Post war collective	29.56	1.44	5
	High rise tower	6.86	0.52	8
	Old detached house	61.96	2.87	5
	Recent detached house	10.71	0.68	6


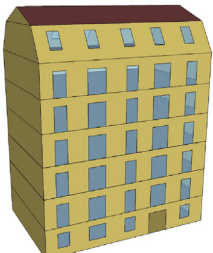

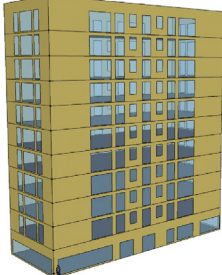

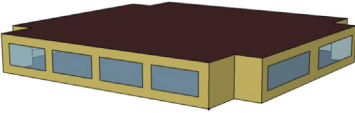

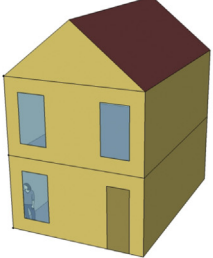

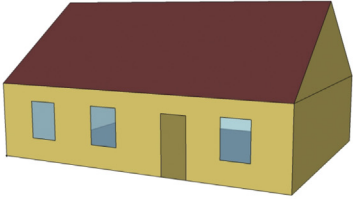
Building name	Typical date	Photography	Detailed model
Historical collective	Before 1900		
Post War collective	1945-1967		
High rise tower	1968-1975		
Old detached house	1950-1973		
Recent detached house	2005		

Fig. 5. Set of representative buildings of the Paris area.

been done with the detailed model used as the reference. The sensitivity of the heating demand has been evaluated for present climate conditions, while the sensitivity of the cooling demand has been evaluated for future climate.

EnergyPlus has the ability to dynamically calculate the infiltration as a function of the wind speed and the air temperature difference between the indoor and the outdoor. Simulations for the historical collective building and the recent detached house using a fixed infiltration rate have been compared to simulations using a dynamic infiltration rate. In this case, the fixed rate was

computed as the annual average of the dynamic rate. The differences between both simulations were low (Table 5) with less than 3 and 0.1 kWh/m²[floor]/year absolute difference for the heating demand in the case of present climate conditions for respectively the historical collective building (4% of the annual heating demand) and the recent detached house (less than 1% of the annual heating demand). For the cooling demand with future climate conditions, the difference was less than 0.3 kWh/m²[floor]/year (2%) for the historical collective building and less than 0.1 kWh/m²[floor]/year (less 1%) for the recent detached house.

Table 7
Comparison of the cooling demand between the simplified and the detailed model simulated with EnergyPlus.

Climate	Building type	Detailed model energy demand kWh/m ² [floor]/year	Absolute difference (simpl.–detailed) kWh/m ² [floor]/year	Relative difference (simpl.–detailed) %
Present climate	Historical collective	5.65	−0.47	−8
	Post war collective	7.36	0.73	10
	High rise tower	7.54	0.84	11
	Old detached house	6.73	1.08	16
	Recent detached house	7.98	0.05	1
Future climate	Historical collective	44.14	−5.20	−12
	Post war collective	61.88	0.68	1
	High rise tower	44.21	2.47	6
	Old detached house	39.80	2.60	7
	Recent detached house	87.07	−1.05	−1

In the house with a pitched roof, the roof-space is generally naturally ventilated by infiltration. Two simulations, one with roof-space ventilation of 0.1 ACH and another without roof space ventilation were compared. The results indicate also a low sensitivity to this ventilation with $-0.22 \text{ kWh/m}^2[\text{floor}]/\text{year}$ of absolute difference for heating (-1%) and $-0.13 \text{ kWh/m}^2[\text{floor}]/\text{year}$ difference (-1%) for the cooling demand (Table 5).

Then, one of the simplifications adopted in TEB is the flat roof shape. Two simulations, one with a flat roof building and the other with the original pitched shape have been compared for the historical collective building and the recent detached house. The differences were respectively of $-1.40 \text{ kWh/m}^2[\text{floor}]/\text{year}$ (-2%) and $0.23 \text{ kWh/m}^2[\text{floor}]/\text{year}$ (less than 1%) for heating. For cooling in future climate conditions, the differences between simulations with and without the flat roof are also very low for both buildings (Table 5).

Finally, the top floor in contact with the roof is generally more exposed to high cooling demand because of the strong influence of the roof. A simulation of the historical collective building with 2 thermal zones (one for the top floor and single one for the other floors) has been compared with a simulation with a single thermal zone. It resulted in differences of $-0.94 \text{ kWh/m}^2[\text{floor}]/\text{year}$ (-1%) and $-0.13 \text{ kWh/m}^2[\text{floor}]/\text{year}$ (-0.7%) respectively for the heating and the cooling demand (Table 5). In order to catch more accurately the thermal stratification that can occur in a 7 floors building, a simulation of the historical collective building with 7 thermal zones (one per floor) has been compared with the single zone simulation. The differences were slightly higher than for the 2 thermal zones representation but remains below 5% of relative difference.

From these comparisons, it has been concluded that the representation of a dynamic infiltration rate, the roof ventilation, a pitched-roof shape and the top floor was not necessary for our application.

Then, the results of the exhaustive comparisons conducted for the 5 representative buildings selected and the 2 climate conditions between DM and SM are presented for heating in

Table 8
Comparison of the heating demand computed with TEB and with EnergyPlus for the detailed model.

Climate	Building type	Absolute difference (simpl.–detailed) kWh/m ² [floor]/year	Relative difference (simpl.–detailed) %
Present climate	Historical collective	−8.46	−11
	Post war collective	−4.98	−4
	High rise tower	−0.80	−2
	Old detached house	19.88	10
	Recent detached house	2.44	5
Future climate	Historical collective	−1.55	−7
	Post war collective	−0.91	−3
	High rise tower	−0.12	−2
	Old detached house	9.54	15
	Recent detached house	1.51	14

Table 6 and for cooling in Table 7. For the heating demand (Table 6), it was found that the absolute differences (absolute values) average $\pm 2.44 \text{ kWh/m}^2$ of floor space for the 5 buildings for the present climate (3%) and $\pm 1.26 \text{ kWh/m}^2$ of floor space for the future climate (5%). The accuracy of the simplified representations is even stronger as the heating demand is important and all differences are lower than 10% of the heating demand of the reference. In the case of the present climate for which the heating demand is predominant, 4 of the 5 buildings are represented by the SM with a difference lower than 5% . These comparisons allow us to conclude that the simplified representation of the buildings meets our precision expectations for the calculation of the heating demand.

Comparisons between DM and SM for the calculation of the cooling demand are presented in Table 7. The differences are slightly higher than for the comparison of the calculations of heating but most of them remain below 10% . In the case of the present climate, the relative differences are the highest (Table 7), but they are not significant since the average of the absolute deviations over the 5 buildings is $\pm 0.63 \text{ kWh/m}^2[\text{floor}]/\text{year}$ (9%). The increase of the relative difference in this case is mainly due to the low level of the air conditioning demand (between 5 and $8 \text{ kWh/m}^2[\text{floor}]/\text{year}$). For the future climate conditions, the air conditioning demand is higher, between 39 and $81 \text{ kWh/m}^2[\text{floor}]/\text{year}$ and in this case, 4 of the 5 buildings are represented with the SM with differences lower than 5% . Overall the 5 buildings, the average absolute deviation is $2.40 \text{ kWh/m}^2[\text{floor}]/\text{year}$ (5%) for these future climate conditions. These comparisons demonstrated that when the cooling demand is significant, a simplified representation can reproduce air conditioning demand applications with an accuracy of $\pm 15\%$.

3.5 Results of the comparison between EnergyPlus and TEB

The comparisons between the heating demand calculated by the simulations of the 5 building types with TEB and the EnergyPlus simulations of the DM are presented in Table 8. For all

Table 9

Comparison of the cooling demand computed with TEB and with EnergyPlus for the detailed model.

Climate	Building type	Absolute difference (simpl.–detailed) kWh/m ² [floor]/year	Relative difference (simpl.–detailed) %
Present climate	Historical collective	–0.72	–13
	Post war collective	0.70	10
	High rise tower	0.92	12
	Old detached house	1.10	14
	Recent detached house	0.74	11
Future climate	Historical collective	–4.88	–11
	Post war collective	4.29	7
	High rise tower	4.58	10
	Old detached house	12.16	14
	Recent detached house	3.08	8

types of building, the average absolute differences are respectively ± 7.31 kWh/m²[floor] per year for the present climate (6%) and ± 2.73 kWh/m²[floor] per year for the future climate (8%). This comparison demonstrated that TEB is able to estimate the heating demand with an accuracy better than 15% in general and better than 10% when this demand is significant.

For the cooling demand, the same comparisons are presented in Table 9. In the case of the present climate for which the cooling demand is low, TEB is able to estimate the cooling demand with absolute differences generally lower than 1 kWh/m²/year (± 0.84 kWh/m²[floor] per year on average over the 5 building types) which results in relative differences always lower than 15% (12% on average). In the case of the future climate for which the cooling demand is the predominant fraction of the energy demand, the absolute difference is generally lower than 5 kWh/m²[floor]/year and the relative difference remains below 15% (± 5.80 kWh/m²/year on average or 10%). This comparison shows that for both climate conditions, TEB is able to reproduce the cooling demand for a variety of building types with a precision better than 15%. In regards to their possible impact on the urban heat island, these differences are low. Indeed, the differences of energy demand presented in this table do not lead to differences of the heat releases in the atmosphere higher than 10 Wm^{-2} while a difference of around 100 Wm^{-2} is necessary to generate an outdoor temperature difference of 1 K [8].

4. Sensitivity to the representation of the building surrounding surface temperature

In TEB, the surface temperatures of a wall's surrounding (road, opposite wall) are explicitly resolved and used in the calculation of the longwave radiation balance. In EnergyPlus, these temperatures are approximated by the air temperature. The sensitivity to this approximation was evaluated with the TEB model. Two sets of simulations were compared: one using the air temperature for calculating the longwave radiation exchange of the wall with its environment such as in EnergyPlus and the other using the temperature of the road and the opposite wall resolved by the model. In an urban environment, the buildings are rarely isolated and the view factors of one wall with the road, with its opposite wall and the sky can present large variations depending on the building plan area density. Consequently, each building defined in this study has been simulated for a set of plan area densities included in an adapted range (Table 10). At the same time, the W_oH ratio has

been adapted in order to preserve the W_oB ratio of the building that fixed the wall surface envelope (Eq. (1)).

The differences of the heating demand between the simulations using the TEB estimates for the surface temperature of the surrounding and the simulations using the air temperature as in EnergyPlus are presented in Fig. 6. They have been calculated for the present climate conditions for which the heating demand is significant. The use of the road and the wall surface temperatures tend to decrease the heating demand for all buildings but the relative difference tends to be small since they are never above 7% in relative value. The differences are stronger for the 3 buildings that have no insulation in the wall construction. Moreover, except for the old detached housing (highest heating demand of the different buildings), the difference remains constant as the street canyon aspect ratio evolves. During the winter period of the year, when the heating demand occurs, the road and the wall surface temperature are frequently in equilibrium with the air temperature. Fig. 7 presents the differences between the road surface temperature and the air canyon temperature for simulations of the post war collective buildings in two different morphological configurations. During the winter period, the median difference between these temperatures is generally lower than 1 K and 50% of the samples are between 0 and 2.5 K. These low differences between the road and the air temperatures can be related to the fact that during this period of the year, the cloudy days with low solar radiation are frequent and that the sun elevation is low and the road is rarely sunlit.

The differences of the cooling demand between the same configurations of simulation have also been evaluated for the possible future climate conditions and are presented in Fig. 8. For this energy demand, the impact of the use of the road and the wall surface temperatures is significant when the canyon aspect ratio is low. In the case of isolated building, the relative differences are between 6 and 20%. As for the heating demand, the impact is stronger as the walls of the buildings are poorly insulated. The use of the calculated road and wall surface temperatures instead of the air temperature tends to increase the cooling demand because these temperatures tend to be higher than the air temperature when the solar radiation is strong. The differences between the road surface temperature and the air temperature, presented in Fig. 7, are for 50% of the samples between 2 and 10K when the canyon aspect ratio is low. When the canyon aspect ratio increases, the relative difference in cooling demand between the two sets of simulation tends to decrease significantly. For the two collective buildings (poorly insulated), the difference vary from 13 to 3%

Table 10

Typical range of the building plan area density of the environment of each building type.

Building type	Historical collective	Post war collective	High rise tower	Old detached house	Recent house
Building plan area density range	0–0.7	0–0.6	0–0.5	0–0.4	0–0.4

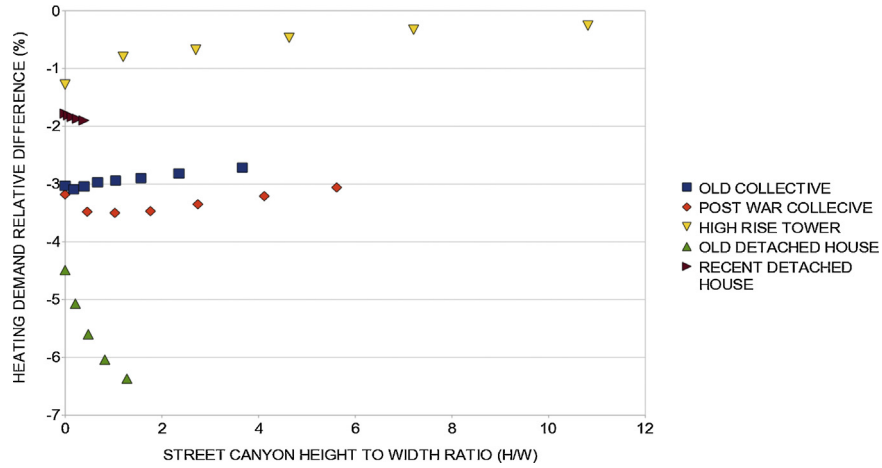


Fig. 6. Heating demand relative differences between simulations using, for the road and the wall surface temperatures, an explicit calculation in the TEB model or the air temperature for different street canyon aspect ratio.

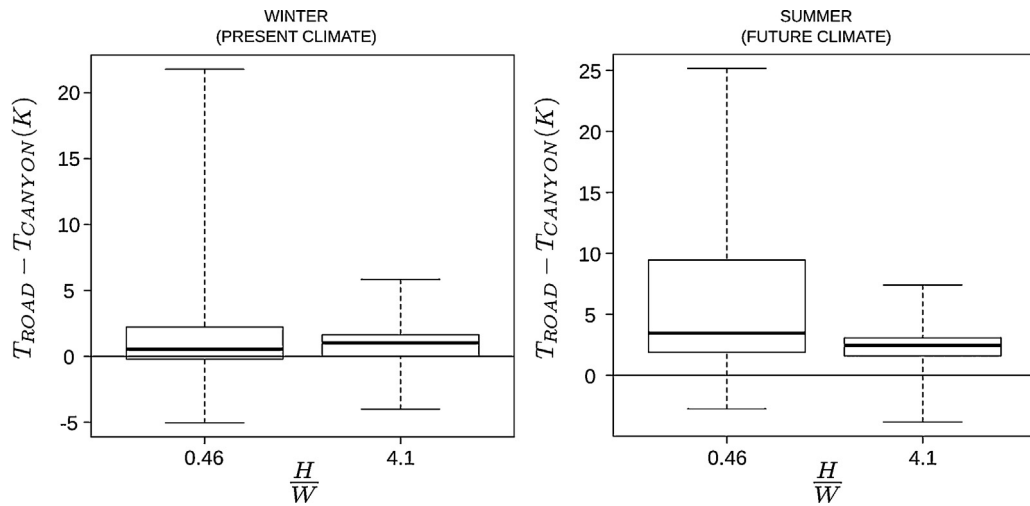


Fig. 7. Boxplots of the differences between the road surface temperature and the air canyon temperature for winter and summer periods for two morphological configurations of the street canyon. The lower and upper level of the bow are respectively the quantile 0.25 and 0.75. The bar inside the box is the median. The bars outside of the box are the minimum and the maximum of the differences.

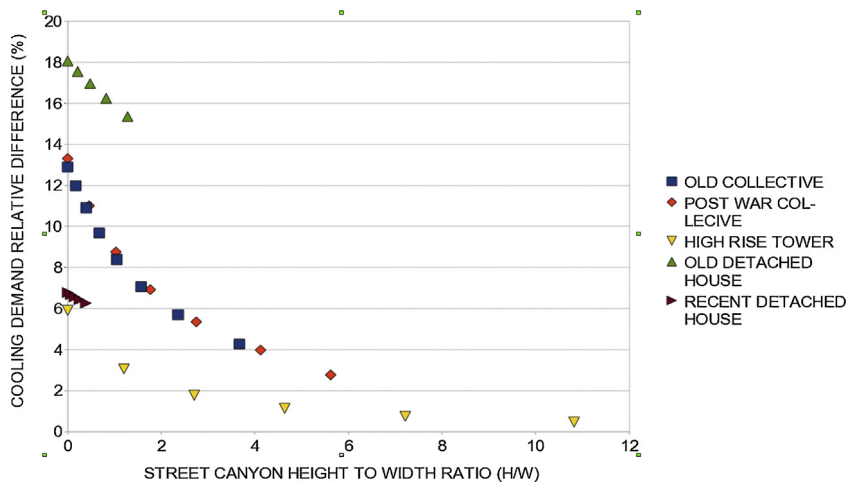


Fig. 8. Cooling demand relative differences between simulations using, for the road and the wall surface temperatures, an explicit calculation in the TEB model or the air temperature for different street canyon aspect ratio.

as the aspect ratio increases to values higher than 5. This is a consequence of the reduction of the solar radiation received by the road and the wall as the canyon aspect ratio increases, which lead to a reduction of the differences between the road (and the wall) surface temperature and the air temperature (Fig. 7).

5. Summary and conclusions

The evaluation of the Building Energy Model (BEM) integrated in the TEB model has been extended for a range of typical buildings representative of Paris and for two contrasted climate conditions. The evaluation has been conducted against the EnergyPlus model, a reference building energy model.

The first step of the evaluation had the objective to verify that the main assumptions adopted in TEB were adapted to all these buildings. Sensitivity analyses to specific levels of details used to represent the buildings have been conducted. Neither a dynamic representation of the infiltration, nor the roof ventilation or shape, nor a larger number of thermal zones inside the building leads to differences that were considered significant for an implementation in an urban canopy model such as the TEB model. Each building has been represented with a detailed model and with a simplified model and the results of the simulation have been compared. On average, the simplified model was able to evaluate the heating and the cooling demand with an accuracy around 1.5 kWh/m²/year for each building energy demand, what is less than 10% of the energy demand.

The second step of the evaluation has been a direct comparison between the results of TEB and EnergyPlus simulations. For these comparisons, TEB adopted the configuration of an isolated building and used the same atmospheric forcing as in EnergyPlus. The analysis led to a revision of the TEB model in order to get satisfying results. Three modifications have been implemented: a simplified anisotropic representation of the sky, a representation of the average effect of the solar incidence angle on the window to compute its optical properties and the calculation of the convective heat transfer coefficients based on an algorithm from EnergyPlus. After these modifications, TEB was able to estimate the heating and the cooling demand with an accuracy of 5 and 3 kWh/m²/year, respectively. These levels of accuracy are better than 15% of the heating or the cooling demand. This comparison has enabled to point out the sensitivity of building energy models to the outdoor energy balance in general. Apart from the convective exchanges, for which a large variety of coefficients exists, the computation of the building's surrounding surface temperature is critical to resolve the longwave radiation balance of the wall and the evaluation of the cooling demand. In the case of isolated buildings with low levels of insulation, simulations that do not resolve explicitly the road surface temperature can underestimate the cooling demand up to 18%. In dense urban environment, these differences tend to be lower but can remain significant. This study highlights the benefits that both communities, building energy and urban climate, can gain by comparing their results.

Acknowledgments

Financial support for this study was provided by the French National Research Agency under the MUSCADE project referenced as ANR-09-VILL-003 and the Ville Numérique project funded by the Ministère de l'Ecologie, du Développement durable et de l'Energie. The researcher from MIT was funded by the Singapore National Research Foundation through the Singapore-MIT Alliance for Research and Technology (SMART) Centre for Environmental Sensing and Modelling (CENSAM).

References

- [1] M. Iamarino, S. Beevers, C.S.B. Grimmond, High-resolution (space, time) anthropogenic heat emissions: London 1970–2025, *Int. J. Climatol.* 32 (2012) 1754–1767.
- [2] G. Pigeon, D. Legain, P. Durand, V. Masson, Anthropogenic heat releases in an old European agglomeration (Toulouse France), *Int. J. Climatol.* 27 (2007) 1969–1981.
- [3] F. Salamanca, A. Martilli, M. Tewari, F. Chen, A study of the urban boundary layer using different urban parameterizations and high-resolution urban canopy parameters with WRF, *J. Appl. Meteor. Climatol.* 50 (2010) 1107–1128.
- [4] Y. Kikegawa, Y. Genchi, H. Kondo, K. Hanaki, Impacts of city-block-scale countermeasures against urban heat-island phenomena upon a building's energy-consumption for air-conditioning, *Appl. Energy* 83 (2006) 649–668.
- [5] J. Adnot et al., Energy Efficiency and Certification of Central Air Conditioners, study for the D.G. Transportation-Energy (DGTREN) of the Commission of the E.U., Final report, Volume 3 (April 2003), available at <http://www.ces.mines-paristech.fr/english/themes/mde/pdf/ECCACfinalvol3.pdf> (consulted 27/02/2014).
- [6] C. de Munck, G. Pigeon, V. Masson, F. Meunier, P. Bousquet, B. Tréméac, M. Merchat, P. Poëuf, C. Marchadier, How much can air conditioning increase air temperatures for a city like Paris, France? *Int. J. Climatol.* 33 (2013) 210–227.
- [7] Y. Ohashi, Y. Genchi, H. Kondo, Y. Kikegawa, H. Yoshikado, Y. Hirano, Influence of air-conditioning waste heat on air temperature in Tokyo during summer: numerical experiments using an urban canopy model coupled with a building energy model, *J. Appl. Meteor. Climatol.* 46 (2007) 66–81.
- [8] B. Bueno, L. Norford, G. Pigeon, R. Britter, A resistance-capacitance network model for the analysis of the interactions between the energy performance of buildings and the urban climate, *Build. Environ.* 54 (2012) 116–125.
- [9] B. Bueno, L. Norford, J. Hidalgo, G. Pigeon, The urban weather generator, *J. Buil. Perform. Simul.* 6 (2013) 269–281.
- [10] L.G. Swan, V.I. Ugursal, Modeling of end-use energy consumption in the residential sector: a review of modeling techniques, *Renew. Sust. Energy Rev.* 13 (8) (2009) 1819–1835.
- [11] M. Kavgić, A. Mavrogianni, D. Mumovic, A. Summerfield, Z. Stevanovic, M. Djurovic-Petrovic, A review of bottom-up building stock models for energy consumption in the residential sector, *Build. Environ.* 45 (7) (2010) 1683–1697.
- [12] V. Masson, A physically-based scheme for the urban energy budget in atmospheric models, *Boundary-Lay. Meteorol.* 94 (2000) 357–397.
- [13] B. Bueno, G. Pigeon, L. Norford, K. Zibouche, C. Marchadier, Development and evaluation of a building energy model integrated in the TEB scheme, *Geosci. Model Dev.* 5 (2012) 433–448.
- [14] V. Masson, C.S.B. Grimmond, T.R. Oke, Evaluation of the town energy balance (TEB) scheme with direct measurements from dry districts in two cities, *J. Appl. Meteorol.* 41 (2002) 1011–1026.
- [15] A. Lemonsu, S. Bélaïr, J. Mailhot, S. Leroyer, Evaluation of the town energy balance model in cold and snowy conditions during the Montreal urban snow experiment 2005, *J. Appl. Meteorol. Climatol.* 49 (2010) 346–362.
- [16] C.S.B. Grimmond, M. Blackett, M.J. Best, J. Barlow, J.J. Baik, S.E. Belcher, S.I. Bohnenstengel, I. Calmet, F. Chen, A. Dandou, K. Fortuniak, M.L. Gouvea, R. Hamdi, M. Hendry, T. Kawai, Y. Kawamoto, H. Kondo, E.S. Krayenhoff, S.H. Lee, T. Loridan, A. Martilli, V. Masson, S. Miao, K. Oleson, G. Pigeon, A. Porson, Y.H. Ryu, F. Salamanca, L. Shashua-Bar, G.J. Steeneveld, M. Tombrou, J. Voogt, D. Young, N. Zhang, The international urban energy balance models comparison project: first results from phase 1, *J. Appl. Meteor. Climatol.* 49 (2010) 1268–1292.
- [17] C.S.B. Grimmond, M. Blackett, M.J. Best, J. Barlow, J.J. Baik, S.E. Belcher, J. Beringer, S.I. Bohnenstengel, I. Calmet, F. Chen, A. Coutts, A. Dandou, K. Fortuniak, M.L. Gouvea, R. Hamdi, M. Hendry, M. Kanda, T. Kawai, Y. Kawamoto, H. Kondo, E.S. Krayenhoff, S.H. Lee, T. Loridan, A. Martilli, V. Masson, S. Miao, K. Oleson, R. Ooka, G. Pigeon, A. Porson, Y.H. Ryu, F. Salamanca, L. Shashua-Bar, G.J. Steeneveld, M. Tombrou, J. Voogt, D. Young, N. Zhang, Initial results from phase 2 of the international urban energy balance model comparison, *Int. J. Climatol.* 31 (2011) 244–272.
- [18] D.B. Crawley, L.K. Lawrie, F.C. Winkelmann, W.F. Buhl, Y.J. Huang, C.O. Pedersen, R.K. Strand, R.J. Liesen, D.E. Fisher, M.J. Witte, J. Glazer, EnergyPlus: creating a new-generation building energy simulation program, *Energy Build.* 33 (2001) 319–331.
- [19] A. Lemonsu, V. Masson, L. Shashua-Bar, E. Erell, D. Pearlmutter, Inclusion of vegetation in the town energy balance model for modelling urban green areas, *Geosci. Model Dev.* 5 (2012) 1377–1393.
- [20] R. Hamdi, V. Masson, Inclusion of a drag approach in the town energy balance (TEB) scheme: offline 1-d validation in a street canyon, *J. Appl. Meteorol. Climatol.* 47 (2008) 2627–2644.
- [21] US Department of Energy, EnergyPlus Engineering Reference, the reference to EnergyPlus Calculation, 2013, pp. 1426, available at <http://apps1.eere.energy.gov/buildings/energyplus/pdfs/engineeringreference.pdf>
- [22] J.A. Palyvos, A survey of wind convection coefficient correlations for building envelope energy system modelling, *Appl. Therm. Eng.* 28 (2008) 801–808.
- [23] T. Defraeye, B. Blocken, J. Carmeliet, Convective heat transfer coefficients for exterior building surfaces: existing correlations and CFD modelling, *Energy Convers. Manage.* 52 (2011) 512–522.

- [24] F.B. Rowley, A.B. Algren, J.L. Blackshaw, Surface, Conductances as affected by air velocity, temperature and character of surface, *ASHRAE Trans.* 36 (1930) 429–446.
- [25] F.B. Rowley, W.A. Eckley, Surface, Coefficients as affected by wind direction, *ASHRAE Trans.* 38 (1932) 33–46.
- [26] P. Mascart, J. Noilhan, H. Giordani, A modified parameterization of flux-profile relationship in the surface layer using different roughness length values for heat and momentum, *Boundary-Lay. Meteorol.* 72 (1995) 331–344.
- [27] ASHRAE, International Weather for Energy Calculations (IWEC Weather Files) Users Manual and CD-ROM, ASHRAE, Atlanta, 2001.
- [28] S. Hallegatte, J.C. Hourcade, P. Ambrosi, Using climate analogues for assessing climate change economic impacts in urban areas, *Clim. Change* 82 (2006) 47–60.
- [29] T.S. Glickman, *Glossary of Meteorology*, 2nd ed., American Meteorological Society, Boston, 2000, pp. 855.
- [30] André Pouget, Amélioration thermique des bâtiments collectifs construits de 1850 à 1974, *Le guide ABC*, Les éditions parisiennes (EDIPA), 2011, pp. 350.
- [31] Atelier Parisien d'Urbanisme (APUR). Consommations d'énergie et émissions de gaz à effet de serre liées au chauffage des résidences principales parisiennes (in French), APUR, December 2007, pp. 44, available at <http://www.apur.org/sites/default/files/documents/246.pdf>
- [32] International Organization for Standardization (ISO), Energy performance of buildings – Calculation of energy use for space heating and cooling, ISO 13790:2008, Geneva, 2008, pp. 162.